Journal of Applied Sciences

ISSN 1812-5654

science alert

ANSInet
an open access publisher
http://ansinet.com

Journal of Applied Sciences 8 (19): 3398-3406, 2008
ISSN 1812-5654

Local Scour at Permeable Spur Dikes

[1]A. Nasrollahi, [2]M. Ghodsian and [2]S.A.A. Salehi Neyshabouri
[1]Department of Civil Engineering, Tarbiat Modares University, Tehran, Iran
[2]Department of Civil Engineering, Water Engineering Research Center,
Tarbiat Modares University, P.O. Box 14115/143, Tehran, Iran

Abstract: In this study, experiments were conducted to investigate the local scour at permeable and impermeable spur dikes extending into the channel at right angle. Based upon dimensional analysis the characteristics of the scour hole at spur dike were correlated to the approach Froude number, the opening ratio of spur dike, the ratio of flow depth to length of spur dike, the ratio of sediment size to length of spur dike and the ratio of channel width to length of spur dike. Also, temporal variations of the depth of scour are presented. The studies have shown that there is considerable reduction in maximum scour depth for permeable spur dikes when compares to those in the corresponding impermeable spur dike situations. Finally, new equations for prediction of the maximum depth of scour and the temporal variations of scour depth around spur dike are presented.

Key words: Scour depth, bed topography, permeability, impermeable, temporal variations

INTRODUCTION

Scour is a natural phenomenon caused by the flow of water in rivers and streams. Scour occurs naturally as a part of the morphological changes of rivers and as a result of man-made structures. Several types of scour can be distinguished.

Generally, the scour process can be split up into different time phases. In the beginning, the development of scour is very fast and eventually an equilibrium situation is reached.

Spur dikes are constructed transverse to the river flow and extend from the bank into the river. Spur dikes, according to the method and type of construction material, are usually classified as permeable, impermeable or semi permeable. It serves one or more of the following functions:

- Training of the stream flow
- Protection of stream bank from erosion
- Improvement of depth for navigation

As a dike constricts the flow it creates backwater effect, which increases with increasing spur dike length. This effect influences the pressure distribution around the spur dike and thereby influences the local flow immediately at the spur dike; i.e., the formation of separation eddies, rollers, various submerged vortices and vertical components of flow at the spur dike (Ettema and Muste, 2004). Due to similarities in the effects of abutment and impermeable spur dike on flow field, the down flow and vortex system at the abutment are shown in Fig. 1. The horseshoe vortex and associated down flow, which are considered to the prime agents causing, scour at abutments and impermeable spur dikes are shown in Fig. 1.

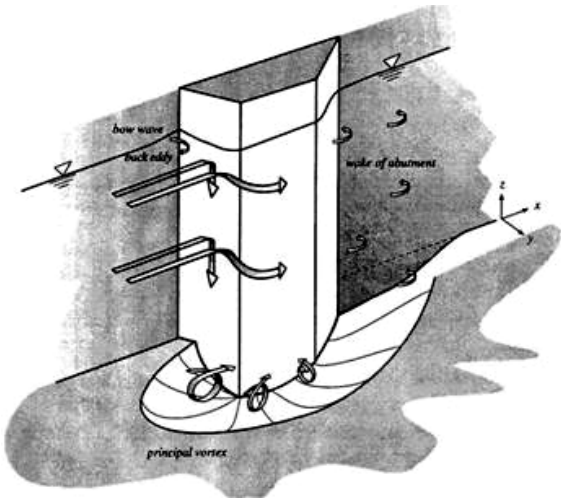

Fig. 1: Vortex systems at an abutment

An important consideration in designing a spur dike is to predict the characteristics of the scour hole produced by flow. Scour depth estimation at spur dike has attracted

Corresponding Author: Ali Nasrollahi, Department of Civil Engineering, Tarbiat Modares University, Tehran, Iran
Tel: +98-21-82884356

considerable research interest and different prediction methods presented by Garde *et al.* (1961), Liu *et al.* (1961), Gill (1972), Neil (1973), Melville (1992, 1997), Lim (1997), Kuhnle *et al.* (1999), Cardoso and Bettess (1999), Melville and Chiew (1999), Ahmed and Rajaratnam (2000), Kothyari and Raju (2001), Radice *et al.* (2002), Kuhnle *et al.* (2002), Ettema and Muste (2004), Dey and Barbhuiya (2004, 2005), Oliveto and Hager (2005) and Fael *et al.* (2006) studied the scour around bridge abutment and impermeable spur dike.

Melville (1992) summarized a large number of experimental results and proposed a design method for maximum scour depth that depends on empirical correction factors for abutment shape, alignment, length and flow depth. In this research, abutment classified as short (L/y<1) or long (L/y>25) and suggested that maximum scour depth was 2L (d_{se} = 2L) for former case and 10y (d_{se} = 10y) for later case. For intermediate abutment length (1<L/y<25) maximum scour depth was proposed to be proportional to y and L ($d_{se} = 2\sqrt{yL}$). Here, y is depth of approach flow and L is abutment length.

In this study, the maximum scour depth at permeable and impermeable spur dike is experimentally investigated for steady uniform flow, close to the initiation of motion of the bed materials. The data analyzed are restricted to a vertical spur dike projecting at an angle of 90° to the main flow direction. Data obtained in the experiments are further used to contribute to a better understanding of the time evolution of local scour at permeable and impermeable spur dike.

FRAMEWORK FOR PRESENT INVESTIGATION

Maximum depth of scour: Typical features of localized scour hole at permeable and impermeable spur dike are shown in Fig. 2.

With reference to Fig. 2, the maximum depth of scour d_{se} for a specified shape of spur dike and for negligible viscous effects can be written as a function of following variables:

$$d_{se} = f_1\left(u, y, \rho_s, \rho, g, d_{50}, B, L, \theta, R, \sigma_g, sh, u_c\right) \quad (1)$$

Where:

u = Mean velocity of approach flow
y = Depth of approach flow
ρ_s = Density of sediment
ρ = Density of water
g = Gravitational acceleration
d_{50} = Mean sediment grain size
B = Width of main channel
L = Length of spur dike

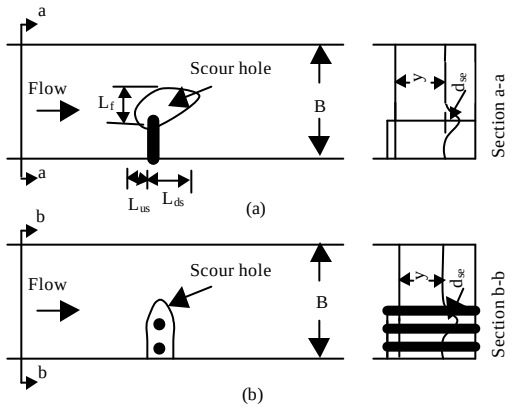

Fig. 2: Schematic view of (a) impermeable and definitions of L_{us}, L_{ds} and L_f and (b) permeable spur dike

θ = Angle of inclination of spur dike to the main flow direction
R = Opening ratio of spur dike
σ = Standard deviation of sediment size distribution
sh = Spur dike shape
u_c = Critical velocity at incipient flow condition

Dimensional analysis of Eq. 1 gives:

$$\frac{d_{se}}{L} = f\left(\frac{u}{\sqrt{gy}}, \frac{L}{d_{50}}, \frac{y}{L}, \frac{B}{L}, \frac{\rho}{\rho_s}, R, \theta, \sigma_g, \frac{u}{u_c}, sh\right) \quad (2)$$

In this study, only vertical wall spur dike with θ = 90° and constant values of ρ/ρ_s and σ_g with $u/u_c \approx 1$ were studied. Therefore, Eq. 2 can be reduced to:

$$\frac{d_{se}}{L} = f\left(\frac{u}{\sqrt{gy}}, \frac{y}{L}, \frac{L}{d_{50}}, R, \frac{B}{L}\right) \quad (3)$$

Following the method proposed by Melville (1992, 1997), Eq. 3 can be evaluated using the experimental data. For this purpose, Eq. 3 can be written as:

$$\frac{d_{se}}{L} = aK_f K_{yL} K_d K_R K_n \quad (4)$$

where, a is empirical constant and the K-factors are expressions describing the influence of parameters appearing in Eq. 3, i.e., K_f accounts for the effect of approach Froude number $F\ (= u/\sqrt{gy})$, K_{yL} accounts for the effects of ratio of spur dike length to the flow depth, K_d accounts for the effect of sediment size d_{50}, K_R accounts for the effect of opening ratio of spur dike R and K_n accounts for the effects of ratio of spur dike length to the channel width.

Time evolution of scour depth: Local scour depth increases progressively with time and finally reaches equilibrium condition. Four phases scour have been identified as the initial, the development, the stabilization and the equilibrium phases. Observation on scour with various bed materials, flow velocities and geometries upstream of the scour hole showed that the relation between the maximum scour depth and time could be summarized in (Hoffmans and Pilarczyk, 1995):

$$\frac{d_s}{d_{se}} = 1 - e^{\ln\left[1-\frac{y}{d_{se}}\right]\left[\frac{t}{t_1}\right]^{\gamma_1}} \quad (5)$$

Where:
d_s = Depth of scour at time t
d_{se} = Equilibrium scour depth
t = Time
t_1 = Time at which the maximum scour depth equals the initial flow depth and γ_1 = 0.2-0.4 for two-dimensional flow

During the development phase of the scour process, that is for $t<t_1$, Eq. 5 can be approximated by:

$$\frac{d_s}{y} = \left(\frac{t}{t_1}\right)^{\gamma_1} \quad (6)$$

$$t_1 = \frac{Ky^2\Delta^{1.7}}{(\alpha u - u_c)^{4.3}} \quad (7)$$

Where:
y = Initial flow depth (m)
K = Coefficient
u = Mean velocity (m sec^{-1})
u_c = Critical mean velocity (m sec^{-1})
α = Coefficient depending on the flow velocity and turbulence intensity (-)
Δ = Relative velocity (-)

Cardoso and Bettess (1999) studied the influence of time on the equilibrium scour depth, d_{se}, at abutments and suggested the following equation:

$$\frac{d_s}{d_{se}} = 1 - \exp\left[-1.025\left(\frac{t}{T}\right)^{0.35}\right] \quad (8)$$

where, T is the time at which d_s = 0.632 ds_e. T can be obtained from the equation:

$$T^* = T\sqrt{g(s-1)d_{50}^3 L^{-2}} \quad (9)$$

Where:

$$T^* = AY^{A_1} \quad (10)$$

Where:
s = Specific density of the bed material
A and A_1 = Constants that depend on the type and geometry of the abutment
$Y = \left[\rho u_*^2\right]/\left[(\gamma_s - \gamma)d_{50}\right]$ = Shields parameter
γ = Specific weight of water
γ_s = Specific weight of the bed material

Because the equilibrium (ultimate) scour d_{se} depends on and $\frac{u}{\sqrt{gy}}, \frac{L}{d_{50}}, \frac{y}{L}, \frac{B}{L}, \frac{\rho}{\rho_s}, R, \theta, \sigma_g, \frac{u}{u_c}$ and sh, it can be assumed that the scour depth at any moment will also depend on the same parameters as well as on t/t_e; that is, d_s will be given by:

$$\frac{d_s}{d_{se}} = f\left(\frac{u}{\sqrt{gy}}, \frac{L}{d_{50}}, \frac{y}{L}, \frac{B}{L}, \frac{\rho}{\rho_s}, R, \theta, \sigma_g, \frac{u}{u_c}, sh, \frac{t}{t_e}\right) \quad (11)$$

For the same conditions where, Eq. 3 applies, Eq. 11 becomes:

$$\frac{d_s}{d_{se}} = f\left(\frac{u}{\sqrt{gy}}, \frac{y}{L}, \frac{L}{d_{50}}, R, \frac{B}{L}, \frac{t}{t_e}\right) \quad (12)$$

where, d_s is scour depth at time t and d_{se} is equilibrium scour depth.

EXPERIMENTS

The experiments were conducted in a horizontal flume of 12 m long, 2 m wide and 0.6 m deep at Tarbiat Modares University. The rather uniform (σ_g = 1.3) non-cohesive sand with d_{50} = 1.3 mm and thickness of 0.45 m was used. The impermeable spur dikes were made of 5 mm thick Perspex with height of 0.7 m. Different lengths of spur dikes i.e., L = 0.25, 0.375, 0.5, 0.625 and 0.75 m were used. The permeable spur dikes were made of brass piles having 5 mm diameter.

Four models of spur dike were used (i.e., with opening ratio of R = 0, 0.3, 0.5 and 0.7). It is clear that R = 0 indicates the impermeable spur dike.
Here, R is defined as:

$$R = \frac{x}{x + D} \quad (13)$$

Where:
x = Distance between piles (edge to edge distance)
D = Diameter of piles used in the permeable spur dike

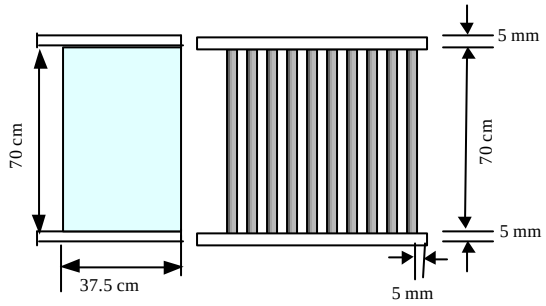

Fig. 3: Permeable and impermeable spur dike

Table 1: Experimental data

Test No.	R	y (mm)	L (mm)	u/u_c	d_{se} (mm)
1	0.00	128	250	1.00	239
2	0.00	128	500	1.00	351
3	0.00	123	375	1.04	303
4	0.00	122	625	1.05	315
5	0.00	122	750	1.05	355
6	0.30	128	250	1.00	106
7	0.30	128	375	1.00	119
8	0.30	130	500	0.98	130
9	0.50	128	250	1.00	36
10	0.50	130	500	0.98	61
11	0.50	127	375	1.00	44
12	0.70	128	375	1.00	20
13	0.70	128	250	1.00	19
14	0.70	127	500	1.00	29

R: Opening ratio of spur dike; y: Depth of approach flow; L: Length of spur dike; u: Mean velocity of approach flow; u_c: Critical mean approach flow velocity at incipient flow condition; d_{se}: Equilibrium scour depth

Figure 3 shows the schematic view of permeable and impermeable spur dikes.

In all the experiments, single spur dike was installed with a 90° angle to the main flow direction. Spur dikes were bolted to the bed of flume and fixed to one side of flume at a distance of 4 m downstream the inflow section. The sediment bed was leveled prior to running each experiment. The experiments were conducted imposing the condition of incipient motion of sediment determined with Shields criterion and checked by observation.

The discharge was kept constant equal to 0.08 $m^3 sec^{-1}$ and measured by a calibrated triangular weir. The depths of flow and scour hole were measured by a point gauge with an accuracy ±0.1 mm.

The flume was first filled slowly with water, thereafter pump was set to a preselected flow rate and the tailgate adjusted for a suitable flow depth. The development of scour hole was monitored and measured until the equilibrium scour condition was established. The equilibrium condition refers to the state that which in these experiments, no further movement of sediment could be detected. The time required to achieve this condition was about 24 h for impermeable spur dike. However, for tests with the permeable spur dikes, equilibrium was attained much faster (about 12 h). The flume was then dewatered and the dimensions and topography of scour hole was measured with a point gauge. The details of the experimental data are shown in Table 1.

RESULTS AND DISCUSSION

General observations: It was observed that immediately after the beginning of each experiment, the scouring was concentrated around the spur dike, starting from the nose of spur dike. Primary vortices and down flow were formed at the nose of spur dike. A separation point was formed at the upstream of the spur dike. As a result a weak vortex is formed upstream of the spur dike. The down flow can generate a strong spiral motion near the bed. By passage of time, the bed materials at the nose of spur dike were thrown to the free surface by boils and bursting motions and are transported downstream by the flow. Bursting motions are very strong at initiation of experiments. The movement of sediment was continued and characterized by trajectories aligned with the flow. This feature indicates the excess mean shear stress due to flow concentration. The sediment movement was characterized by impulsive gusts which, due to complex nature of vortex structure, throw the grains away from the spur dike.

It was observed that the maximum depth of scour in most of the impermeable spur dike cases occurs at the nose of spur dike. While in the case of permeable spur dike the maximum depth of scour occurs almost uniformly all around the spur dike. Moreover, the volume of the scoured material was found to be higher in the case of impermeable spur dike. The bar like deposits downstream of the spur dike was found to be generally inclined to the direction of flow. Typical bed topography around permeable and impermeable spur dikes is shown in Fig. 4 and 5 for $u/u_c = 1.0$.

It is interesting to note that permeability of spur dike have considerable influence in reducing the maximum depth of scour. The larger the opening ratio, R, the greater is the reduction of maximum scour from the corresponding impermeable spur dike.

Maximum depth of scour: Under clear water conditions, scour depth increased with increasing flow velocity and the maximum depth of scour occurs at the initiation of sediment motion. The parameter $u/\sqrt{gy}$ can be written as u/u_c which is a measure of flow intensity and indicates whether sediment motion occurs or not.

The relation presented by Melville (1992) specifically developed for local scour at bridge abutments. In many situations, local scour at bridge abutments and spur dikes is very similar. As mentioned before, present data was analyzed using the method presented by Melville (1992).

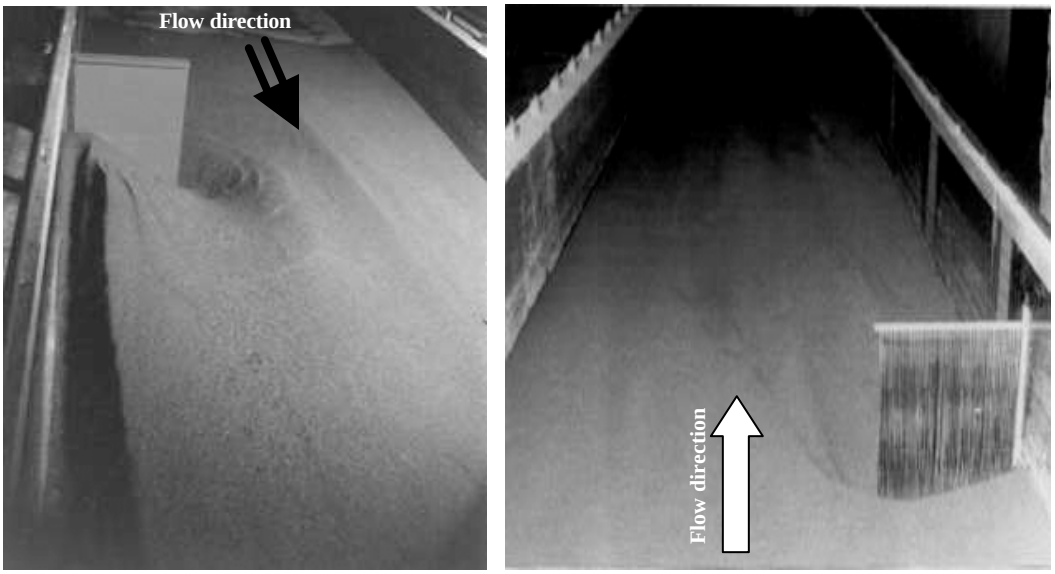

Fig. 4: Bed topography with d_{50} = 1.3 mm, u/u_c = 1.0 and L/y = 3.91, (a) Impermeable spur dike and (b) Permeable spur dike (R = 30%)

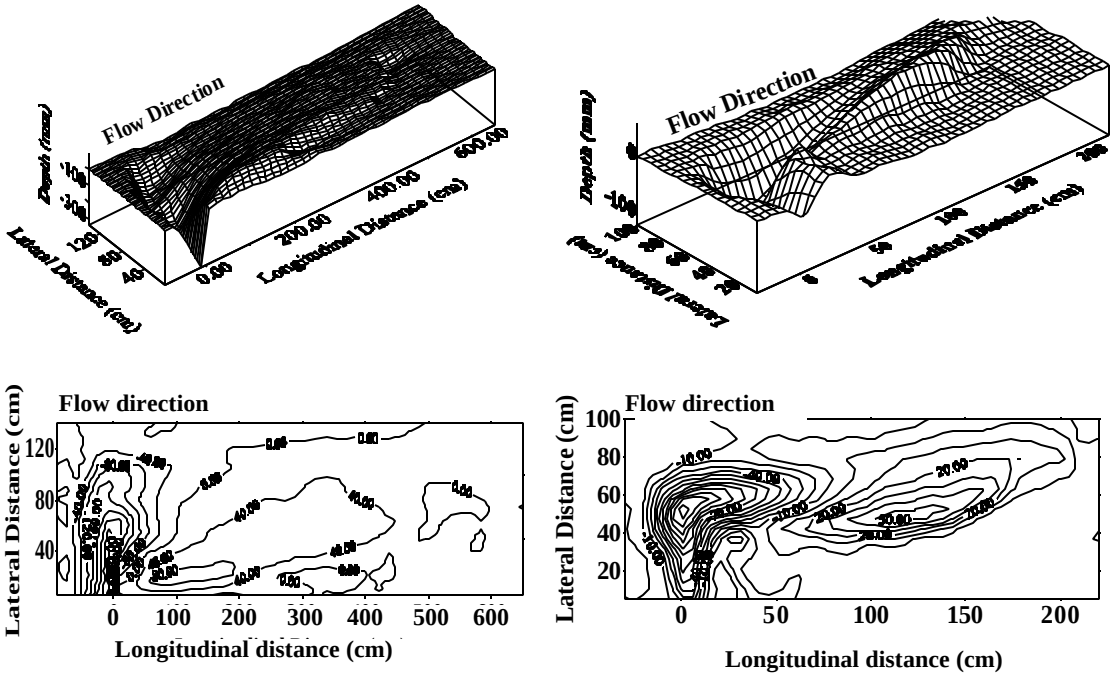

Fig. 5: Typical bed topography around spur dikes with d_{50} = 1.3 mm, u/u_c = 1.0 and L/y = 3.91, (a) Impermeable spur dike and (b) Permeable spur dike (R = 30%)

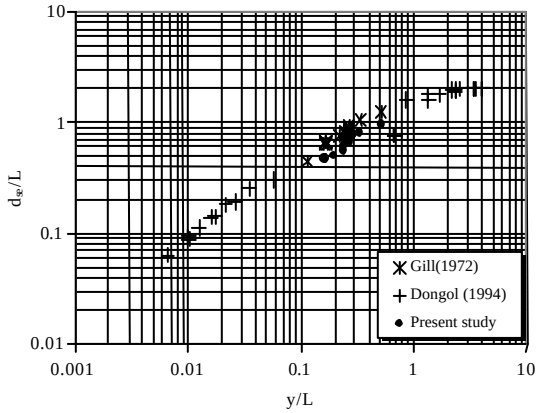

Fig. 6: Effects of the ratio of the flow depth to spur dike length on scour depth

In this study, experimental data from impermeable spur dikes were used as a standard with the K_M factor developed to allow reasonable scour predictions for other conditions. Since, the present study are under the condition of $u/u_c \approx 1$, therefore, $K_f = 1$. Figure 6 shows the variation of d_{se}/L with y/L for impermeable spur dike ($K_R = 1$) using the present data and data of Gill (1972) and Dongol (1994). As can be shown in Fig. 6, the maximum local scour depth increases as the ratio of the flow depth to spur dike length increases. It is also seen that present data lies in the range of intermediate abutment or spur dike ($1<L/y<25$). The following best-fit equation is obtained for d_{se}/L with regression coefficient of $R^2 = 0.9$:

$$d_{se}/L = 1.325\sqrt{y/L} \qquad \text{for } 1<L/y<25 \qquad (14)$$

Therefore, $K_{yL} = 1.325\sqrt{y/L}$

Melville (1992) proposed that K_d be taken as unity, for $L/d_{50}>50$. Since present experimental data lies in this range of L/d_{50}, therefore, $K_d = 1$ is considered.

In order to consider the effect of opening ratio, K_R is defined as the ratio of d_{se}/L with particular opening ratio in a permeable spur dike to that for impermeable spur dike. In this section, the set of experiment from impermeable spur dikes (R = 0) were used as a standard.

Figure 7 displays the influence of opening ratio on scour depth. As can be seen in this figure, the maximum scour depth increases as opening ratio decreases. This is due to its effect on the shear stress around the spur dike. The larger the opening ratio, R, the greater is the reduction of maximum scour from the corresponding impermeable spur dike. The reduction in shear stress due to permeability in a spur dike reflects a reduction in

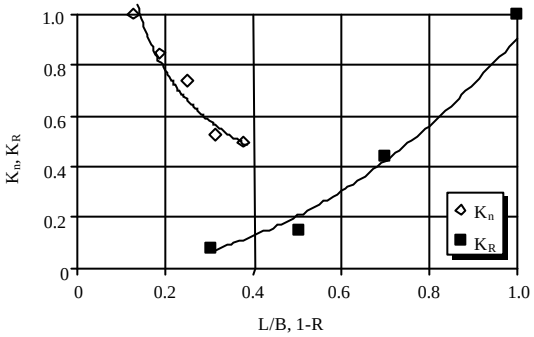

Fig. 7: Effect of contraction ratio and opening ratio on scour depth

particle movement and hence reduced scour in permeable spur dike. The following best fit equation (with $R^2 = 0.98$) is obtained for K_R.

$$K_R = 0.96\,(1-R)^2 \qquad (15)$$

Figure 7 also shows the variation of K_n with L/B for impermeable spur dike. In order to consider the effect of L/B, K_n is defined as the ratio of d_{se}/L with particular L/B in a impermeable spur dike to that for impermeable spur dike with smallest value of L/B (i.e., L/B = 12.5%). It is seen that this effective term decreases as L/B increases. In other words, the maximum scour depth decreases as length of spur dike increases while channel width is fixed. The following equation fit the data with $R^2 = 0.90$.

$$K_n = 0.34\left(\frac{L}{B}\right)^{-0.5} \qquad (16)$$

Further it was found that a = 1.19. Thus, substituting Eq. 14-16 and the value of a in Eq. 4 and keeping in mind that $K_d = 1$ and $K_f = 1$, to get:

$$\frac{d_{se}}{L} = 0.51\left(\frac{y}{L}\right)^{0.5}\left(\frac{L}{B}\right)^{-0.5}(1-R)^2 \qquad (17)$$

Figure 8 shows the comparison of computed values of relative scour depth $(d_{se}/L)_c$ using Eq. 17 with measured values of relative scour depth $(d_{se}/L)_m$. In order to evaluate the accuracy of Eq. 17, the experimental data of Liu *et al.* (1961), Gill (1972), Garde *et al.* (1961) and Dongol (1994) are also plotted in Fig. 8. Considering the nature of the problem, the agreement is acceptable.

Temporal variations of scour depth: During experiments, the local scour process was monitored and scour depths were measured. It was observed that immediately after the

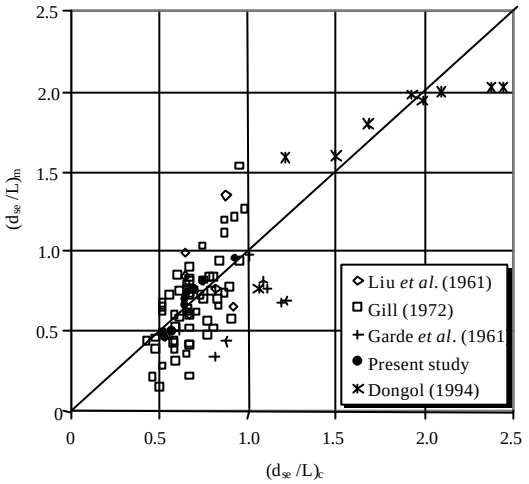

Fig. 8: Comparison of computed and measured relative scour depth

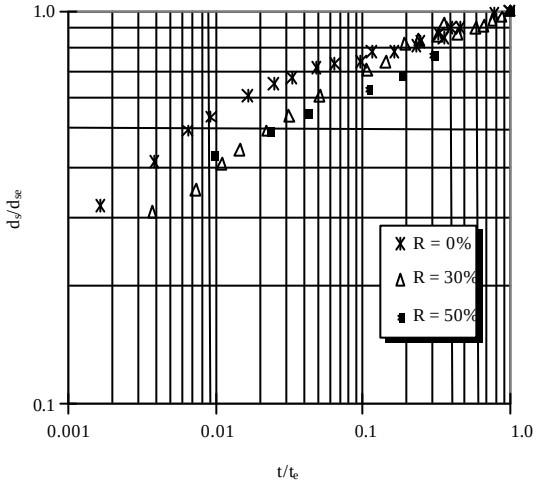

Fig. 10: Temporal development of local scour (L/y= 4)

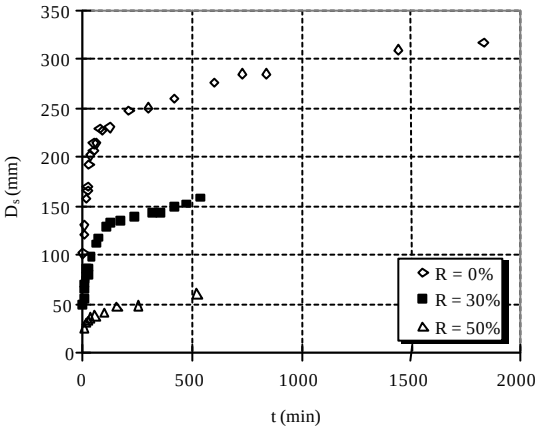

Fig. 9: Time evolution of scour depth (L/y= 4)

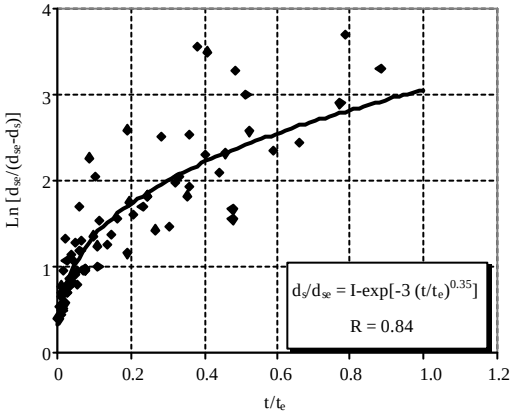

Fig. 11: Time evolution of scour depth in coordinates adopted by whitehouse

beginning of an experiment, the scouring was concentrated at the spur dike side, starting from the nose of spur dike. The movement of sediment was continued and characterized by trajectories aligned with the flow. As the process continues, the scour hole moves towards the flume wall.

Typical evolution of the scour depth with time is shown in Fig. 9 for spur dike with opening ratio 0, 30 and 50%. For tests 1-5 (Table 1), corresponding to the impermeable spur dikes, the scour depths evolve at a decreasing rate with time, reaching equilibrium many hours after the beginning of the tests. For tests with the permeable spur dikes, equilibrium was attained much faster. This may be associated with the fact that vertical slots (gaps) in the body of permeable spur dikes which enable a part of the water flow to pass through their span length, (Fig. 3), thereby shear stress around the permeable spur dike decreases.

Figure 10 shows a temporal variation of scour depth for L/y = 4. This figure shows that about 80% of the maximum scour depth is developed in a time varying from 5% to almost 50% of the maximum time. This figure also shows that at the impermeable spur dike amount of scour in the initial phase is greater than spur dike with opening ratio 0.3 and 0.5. It was found that the effects of R and L/y are of secondary importance and can be neglected in the analysis.

In Fig. 11, the values of $\ln(d_{se}/(d_{se}-d_s))$ are plotted versus t/t_e in the framework of the model used by Whitehouse. The best-fit equation describing the temporal variations of scour was obtained as:

$$\frac{d_s}{d_{se}} = 1 - \exp\left[-3\left(\frac{t}{t_e}\right)^{0.35}\right] \quad (18)$$

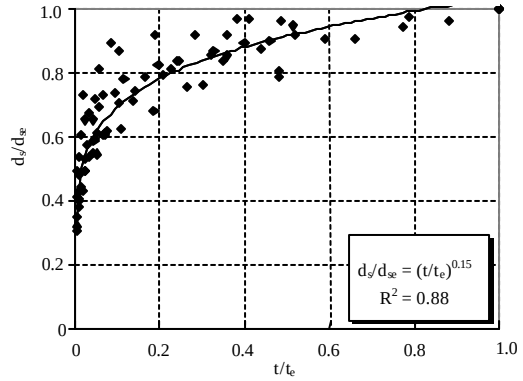

Fig. 12: Temporal variation of scour depth

This is similar to equation developed by Cardoso and Bettess (1999). It should be noted that the constant 0.35 is same as that obtained by Cardoso and Bettess (1999). However, the constant 3 is different from that obtained by these investigators. It is obvious that the data was very scattered from the best-fit line.

In order to have better equation, the data shown in Fig. 11 are also shown in Fig. 12. This figure shows the variations of d_s/d_{se} with t/t_e. The following best fit equation was obtained, which is better than Eq. 18:

$$\frac{d_s}{d_{se}} = \left(\frac{t}{t_e}\right)^{0.15} \quad (19)$$

Thus for present data the above equation is better than the equations obtained by other investigators.

CONCLUSION

Based on the results of this experimental study the following conclusions may be derived:

- The maximum scour depth at permeable and impermeable spur dikes is function of the opening ratio of spur dike, the ratio of flow depth to spur dike length and the ratio of flow depth to length of spur dike
- With increasing the opening ratio of spur dike, the maximum scour depth decreases
- The correction terms for the maximum scour depth are introduced
- New equations for estimation of the maximum scour depth and temporal variation of scour depth in uniform sediment are developed and tested
- There is considerable reduction in maximum scour depth for permeable spur dikes when compares to those in the corresponding impermeable spur dike situations
- Permeable spur dikes could help to increase the safety of the polders behind dikes

NOTATIONS

a	=	Empirical constant
A and A_1	=	Coefficients that depend on geometry of obstacle
B	=	Width of main channel
D	=	Diameter of piles used in the permeable spur dike
d_{50}	=	Mean sediment grain size
d_{se}	=	Equilibrium scour depth
d_s	=	Scour depth at time t
g	=	Gravitational acceleration
K_I	=	Effective terms
K_1 and K_2	=	Coefficients of Ettema's model
L	=	Length of spur dike
L_{ds}	=	Maximum length of scour hole downstream of spur dike
L_f	=	Maximum width of scour hole in front of spur dike
L_{us}	=	Maximum length of scour hole upstream of spur dike
R	=	Opening ratio of spur dike
sh	=	Spur dike shape
s	=	Specific density of the bed material
t	=	Time
t_1	=	time at which the maximum scour depth equals the initial flow depth
t_e	=	Time to develop the equilibrium depth of scour
T	=	Time scale
T*	=	Nondimensional form of time scale T
u	=	Mean velocity of approach flow
u_c	=	Critical mean approach flow velocity at incipient flow condition
u_*	=	Shear velocity
u_*c	=	Critical shear velocity for incipient motion
x	=	Distance between piles (edge to edge distance)
y	=	Depth of approach flow
Y	=	Shields parameter
γ_1	=	Coefficient (dimensionless)
γ	=	Specific weight of water
γ_s	=	Specific weight of the bed material
θ	=	Angle of inclination of spur dike to the main flow direction
ρ	=	Density of water
ρ_s	=	Density of sediment
σ_g	=	Standard deviation of sediment size distribution
υ	=	Kinematic viscosity

REFERENCES

Ahmed, F. and N. Rajaratnam, 2000. Observations on flow around bridge abutment. J. Eng. Mech., 126: 51-59.

Cardoso, A.H. and R. Bettess, 1999. Effect of time and channel geometry on scour at bridge abutments. J. Hydr. Eng. ASCE., 124: 388-399.

Dey, S. and A.K. Barbhuiya, 2004. Clear-water scour at abutments in thinly armored beds. J. Hydr. Eng. ASCE., 130: 622-634.

Dey, S. and A.K. Barbhuiya, 2005. Time variation of scour at abutments. J. Hyd. Eng., 131: 11-23.

Dongol, D.M.S., 1994. Local Scour at Bridge Abutments. 1st Edn., University of Auckland, New Zealand, ASIN: B0018Q643W .

Ettema, R. and M. Muste, 2004. Scale effects in flume experiments on flow around a spur dike in flat bed channel. J. Hydr. Eng. ASCE., 130: 635-646.

Fael, C.M.S., G. Simarro-Grande, J.P. Martin-Vide and A. H. Cardoso, 2006. Local scour at vertical-wall abutments under clear-water flow conditions. Water Resou. Res., 42: W10408-W10408.

Garde, R.J., K. Subramanya and K.O. Nambudripad, 1961. Study of scour around spur dikes. J. Hydr. Div. ASCE., 87: 23-38.

Gill, M.A., 1972. Erosion of sand bed around spur dikes. J. Hydr. Div. ASCE., 98: 1587-1602.

Hoffmans, G.J.C.M. and K.W. Pilarczyk, 1995. Local scour downstream of hydraulic structures. J. Hyd. Eng. ASCE., 121: 326-340.

Kothyari, U.C. and K.G.R. Raju, 2001. Scour around spur dikes and bridge abutments. J. Hyd. Res., 39: 367-374.

Kuhnle, R.A., C.V. Alonso and F.D. Shields, 1999. Geometry of scour holes associated with 90o spur dikes. J. Hydr. Eng. ASCE., 125: 972-978.

Kuhnle, R.A., C.V. Alonso and F. D. Shields, 2002. Local Scour Associated with Angled Spur Dikes. J. Hydr. Eng. ASCE., 128: 1087-1093.

Lim, S.Y., 1997. Equilibrium clear-water scour around an abutment. J. Hydr. Eng. ASCE., 123: 237-243.

Liu, H.K., F.M. Change and M.M. Skinner, 1961. Effect of bridge constriction on scour and backwater. Report CER60-HKL22, Depatment of Civil Engineering, Colorado State University

Melville, B.W., 1992. Local scour at bridge abutments. J. Hyd. Eng. ASCE., 118: 615-631.

Melville, B.W., 1997. Pier and abutment scour- integrated approach. J. Hyd. Eng. ASCE., 123: 125-136.

Melville, B.W. and Y.M. Cheiw, 1999. Time scale for local scour at bridge piers. J. Hyd. Eng. ASCE., 125: 59-65.

Neil, C.R., 1973. Guide to Bridge Hydraulics. 1st Edn., University of Toronto Press, Canada, ISBN: 0727732625 .

Oliveto, G. and W.H. Hager, 2005. Further results to time-dependent local scour at bridge elements. J. Hyd. Eng. ASCE., 131: 97-105.

Radice, A., S. Franzetti and F. Ballio, 2002. Local scour at bridge abutments. Proceeding of International Conference on Fluvial Hydraulics, River Flow 2002, September 4-6, Louvain-LA-Neuve, pp: 1059-1068.